The Stoichiometry of Trimeric SIV Glycoprotein Interaction with CD4 Differs from That of Anti-envelope Antibody Fab Fragments

THE JOURNAL OF BIOLOGICAL CHEMISTRY
Vol. 276, No. 46, Issue of November 16, pp. 42667–42676, 2001

Printed in U.S.A.

The Stoichiometry of Trimeric SIV Glycoprotein Interaction with CD4 Differs from That of Anti-envelope Antibody Fab Fragments*

Received for publication, May 8, 2001, and in revised form, August 29, 2001
Published, JBC Papers in Press, September 5, 2001, DOI 10.1074/jbc.M104166200

Mikyung Kim‡, Bing Chen§, Rebecca E. Hussey‡, Yasmin Chishti‡, David Montefiori¶, James A. Hoxie‖, Olwyn Byron, Gordon Campbell**, Stephen C. Harrison§, and Ellis L. Reinherz‡ ‡‡**

*From the ‡Laboratory of Immunobiology, Dana-Farber Cancer Institute and Department of Medicine, Harvard Medical School, Boston, Massachusetts 02115, the §Laboratory of Molecular Medicine, The Children's Hospital, Howard Hughes Medical Institute, Boston, Massachusetts 02115, the ¶Department of Surgery, Duke University Medical School, Durham, North Carolina 27710, the ‖Department of Medicine, University of Pennsylvania, Philadelphia, Pennsylvania 19104, and the **Division of Infection and Immunity, Institute of Biomedical and Life Sciences, University of Glasgow, Glasgow G12 8QQ, United Kingdom*

Human and simian immunodeficiency viruses infect host lymphoid cells by binding CD4 molecules via their gp160 envelope glycoproteins. Biochemical studies on recombinant SIVmac32H (pJ5) envelope ectodomain gp140 precursor protein show that the envelope is a trimer. Using size exclusion chromatography, quantitative amino acid analysis, analytical ultracentrifugation, and CD4-based competition assay, we demonstrate that the stoichiometry of CD4 receptor-oligomeric envelope interaction is 1:1. By contrast, Fab fragments of both neutralizing and non-neutralizing monoclonal antibodies bind at a 3:1 ratio. Thus, despite displaying equivalent CD4 binding sites on each of the three gp140 protomers within an uncleaved trimer, only one site binds the soluble 4-domain human CD4 extracellular segment. The anti-cooperativity and the faster k_{off} of gp140 trimer:CD4 *versus* gp120 monomer:CD4 interaction suggest that CD4-induced conformational change is impeded in the intact envelope. The implications of these findings for immunity against human immunodeficiency virus and simian immunodeficiency virus are discussed.

The acquired immunodeficiency syndrome (AIDS)[1] in humans and monkeys is caused, respectively, by the human immunodeficiency viruses (HIV1 and HIV2) and the related primate lentiviruses, designated simian immunodeficiency viruses (SIVs) (1–7). Both HIV and SIV utilize CD4 molecules as cellular receptors (8–13). Moreover, both viruses have a related, trimeric envelope spike protein containing non-covalently associated gp120 and gp41 glycoprotein fragments derived from a posttranslationally cleaved precursor polypeptide (14, 15). The envelope glycoproteins are essential for viral infectivity and pathogenesis.

The HIV and SIV envelope trimers have at least three conformational states: an unliganded state found on the surface of mature virions, a CD4-liganded state, and an end-product state in which the gp120 fragments have dissociated from the gp41 trimers and the gp41 portions have rearranged (16–18). The transition to this final state is triggered by binding of the viral co-receptor, a member of the chemokine-receptor family (19, 20). There are likely to be intermediate states of varying stability in the transitions between the conformations just listed. Cleavage of the envelope precursor (gp160) is required for the transition between the last two states and may be important for the first transition as well. CD4 binds more weakly to envelope trimers from fresh viral isolates than to the gp120 monomers derived from them, consistent with the notion that the initial state of the trimer restrains its gp120 moieties in a low-affinity conformation and with the observations that CD4 binding induces a structural transition (21, 22).

Structures have been determined for the gp41 ectodomain, in a state that probably corresponds to the final conformational rearrangement (23–25) and for a truncated, monomeric HIV1 gp120 complexed with CD4 and a monoclonal Fab that covers the co-receptor site (26). The latter structure is presumably also in a state similar to the one found after dissociation of the gp120 fragment from the envelope trimer (16, 17). The structure of the initial state of the gp160 (or gp120/gp41) trimer is not known. Models derived from the structure of free gp120 in complex with CD4 yield plausible approximations, but these are limited by uncertainties concerning conformational rearrangements (27).

In this paper, experiments were designed to analyze properties of the SIVmac32H envelope protein ectodomain gp140, overexpressed in a recombinant system. We have recently reported results from chemical cross-linking, analytical ultracentrifugation, and mass spectrometry that demonstrate that the secreted recombinant protein, modified to render it unsusceptible to the processing cleavage, is a trimer (28). Stably trimeric SIV envelope protein offers an opportunity to determine biochemical correlates of its various states. We describe here the kinetics of CD4 binding to trimeric gp140 *versus* monomeric gp120 and the stoichiometry of the CD4 interaction for each. We also report the binding properties of Fab fragments from neutralizing and non-neutralizing monoclonal antibodies (mAbs). We show that only one CD4 molecule binds to an uncleaved trimer, while both neutralizing and non-neutralizing Fabs bind with a stoichiometry of one Fab per gp120/gp41 subunit.

* This work was supported by Novel HIV Therapy-ICHP Grant AI43649 (to E. L. R. and S. C. H.), an Innovation Grant (to S. C. H.), the Howard Hughes Medical Institute, and National Institutes of Health Grant AI85343 (to D. M.). The costs of publication of this article were defrayed in part by the payment of page charges. This article must therefore be hereby marked "*advertisement*" in accordance with 18 U.S.C. Section 1734 solely to indicate this fact.

‡‡ To whom correspondence should be addressed: Dana-Farber Cancer Inst., 44 Binney St., Boston, MA 02115; Tel.: 617-632-3412; Fax: 617-632-3351; E-mail: ellis_reinherz@dfci.harvard.edu.

[1] The abbreviations used are: AIDS, acquired immunodeficiency syndrome; HIV, human immunodeficiency virus; SIV, simian immunodeficiency virus; mAb, monoclonal antibody; PBS, phosphate-buffered saline; RAM Fc, rabbit anti-mouse Fc; AAA, amino acid analysis; PAGE, polyacrylamide gel electrophoresis; Ve, elution volume.

EXPERIMENTAL PROCEDURES

Expression and Purification of SIV gp140, gp140 Variants, gp120, and Human CD4—SIV gp140 and variants from SIVmac32H (pJ5) were expressed in Lec3.2.8.1 cells using the pEE14 expression system as previously described and referred to as gp160e (28, 29). To produce SIV gp120, the tissue plasminogen activator leader sequence was fused with the N terminus of SIV gp120. SIV gp120 was amplified by polymerase chain reaction, gel purified, and cloned into pEE14 digested with *Xba*I and *Eco*RI to generate pSG120 encoding amino acids 1–524. The Lec3.2.8.1 supernatants containing gp140 were filtered (Corning, 0.22 μm) and passed over a mAb 17A11 (30) affinity column (5-ml bed volume) with a flow rate of 0.5 ml/min. The mAb 17A11 was coupled at 5 mg/ml to Gamma Bind Plus-Sepharose beads (Amersham Pharmacia Biotech) via cross-linking with dimethyl pimelimidate. After extensive washing with PBS, the bound gp140 protein was eluted with low pH buffer (500 mM acetic acid, pH 3.0), and peak fractions were immediately adjusted to pH 7.2 using 1 M Tris, pH 9.0, pooled, concentrated to 2 ml with an Amicon Centriprep-50 concentrator, and loaded onto a 1.6 $\times$ 60-cm Superdex 200 column (Amersham Pharmacia Biotech) equilibrated with 20 mM Tris, and 200 mM NaCl, pH 8.0. SIV gp140 (ΔV1V2), gp140 (ΔV1V2V3), gp140C1, gp140C2, and gp120 proteins were purified following the same procedure. For purification of human s4CD4, Chinese hamster ovary cell-secreted s4CD4 protein (31) was purified using a 19Thy5D7 mAb affinity column chromatography and then sized by a Superdex 75 gel filtration column equilibrated with 20 mM Hepes, and 100 mM NaCl, pH 7.0, to remove any aggregates. s2CD4, an *Escherichia coli* protein comprising amino acids 1–183 of hCD4, was produced, refolded, and purified as described (32).

Surface Plasmon Resonance Binding Analyses—All experiments were performed with a BIACORE 1000 instrument (Biacore, Piscataway, NJ) at 25 °C in HBS running buffer (150 mM NaCl, 3.4 mM EDTA, 0.005% surfactant P-20, 10 mM Hepes, pH 7.4). For epitope mapping of soluble gp140, the antigenic determinants recognized on the gp140 molecule in solution were mapped using a two-site assay. Each mAb (0.6 μM) was captured by RAM Fc covalently bound to the carboxylated dextran matrix by an amine-coupling kit (Biacore) at a flow rate of 5 μl/min. The unoccupied sites of RAM Fc were blocked with 5 μl of an unrelated mAb to avoid binding of the second mAb to unoccupied ligand sites. In the two-step procedure, gp140 (0.2–2 μM) was injected followed by injection of the second mAb (0.6 μM) at a flow rate of 5 μl/min. For determination of the mAb reactivity, mAbs were captured by RAM Fc and then exposed to analyte containing gp140, gp140 (ΔV1V2), gp140 (ΔV1V2V3), or a chimeric HIV gp120-SIV gp41 fusion protein (kind gift of George Gao, Children's Hospital, Boston, MA). RAM Fc serves as a convenient capture reagent for mAbs used in the kinetic experiments. Analyte containing gp140 at eight different concentrations (5–300 nM) was passed over each mAb surface. In parallel studies, s4CD4 was added at a 20-fold molar excess to gp140 overnight before measuring binding. Binding and dissociation were measured for 240 s each at a flow rate of 50 μl/min. The sensor surface was regenerated between each binding reaction by using two washes of 0.1 M HCl for 15 s at 100 μl/min.

For the kinetics of gp140 and gp120 binding to s4CD4, CD4 was coupled to a CM5 chip surface using standard amine-coupling procedures. The immobilization level was 500–1000 response units for s4CD4. All experiments were performed on three surfaces of different ligand densities in HBS buffer at 25 °C. Association was measured by passing various concentrations of gp140 or gp120 (50 nM to 4 μM) over each ligand surface at a flow rate of 50–100 μl/min. The sensor surface was regenerated between each binding reaction by using two washes of 100 μM HCl for 6 s at 100 μl/min. Identical injections over blank surfaces were subtracted from the data for kinetic data analysis. Binding kinetics were evaluated in a 1:1 binding model.

Stoichiometry Measurements—The protein concentrations of gp140 monomer, gp120, and s4CD4 were determined at 280 nm using the theoretical extinction coefficients 181540 M^{-1} cm^{-1}, 126250 M^{-1} cm^{-1} and 62060 M^{-1} cm^{-1}, respectively, based on primary amino acid sequence. For the SIV envelope, this result was in excellent agreement with the Bio-Rad version of the Bradford dye binding assay. For analysis of stoichiometry by gel filtration, purified trimeric gp140 was mixed with Fab fragments at ratios from 1:1 to 1:5 (mol:mol). The protein concentration of each of the two component mixtures prior to purification ranged from 2–12 mg/ml. Each mixture was incubated overnight at 4 °C and subsequently analyzed by gel filtration using a Superdex 200 column equilibrated with 20 mM Tris-HCl, and 200 mM NaCl, pH 8.0, at a flow rate of 0.7 ml/min controlled by the AKTA FPLC (Amersham Pharmacia Biotech).

Neutralization Assay—All neutralization experiments were performed with purified mAbs. SIVmac239 and SIVsmH-4 are molecularly cloned viruses, whereas SIV/DeltaB670 and SIVmac251 (mac32H (pJ5) equivalent) are uncloned virus stocks. Virus stocks were produced in H9 cells except for SIVmac239, which was produced in human peripheral blood mononuclear cells. The SIVmac251 stock was extensively passaged in T cell lines (33). Cell-free virus (50 μl containing 0.5–1 ng of p27) was added to multiple dilutions of mAbs in 100 μl of growth medium in triplicate wells of 96-well microdilution plates and incubated at 37 °C for 30 min before addition of CEMx174 cells (10^5 cells in 100 μl/well). Cell densities were reduced severalfold, and medium was replaced after 3 days of incubation. The incubation was continued until virus-induced syncytium formation and cell killing were observed microscopically in wells incubated in the absence of mAbs. Neutralization was measured by staining viable cells with Finter's neutral red in poly-L-lysine-coated plates. Neutral red uptake by CEMx174 cells is linear from 3.1×10^4 to 5×10^5 viable cells/well corresponding to A_{540} values of 0.25–1.6. Percent protection was calculated by the difference in absorption between test wells (cell plus mAb plus virus) and virus control wells (cells plus virus), divided by the difference in absorption between cell control wells (cells) and virus control wells. The ID_{50} is defined as the concentration of mAb necessary to protect cells from virus-induced death (to a level of 50%).

Amino Acid Analysis—For amino acid analysis (AAA), 200 μg of purified gp140 was incubated with s4CD4 to 30-fold molar excess overnight at 4 °C and then loaded onto a Superdex 200 HR 10/30 column controlled by an AKTA FPLC (Amersham Pharmacia Biotech). The column was equilibrated with 20 mM Tris-HCl, and 200 mM NaCl, pH 8.0, at a flow rate of 0.7 ml/min. The peak fractions containing the gp140-s4CD4 complex were separated from free s4CD4, pooled, concentrated, and buffer-exchanged into PBS for AAA. These samples as well as purified gp140 alone and purified s4CD4 alone were individually hydrolyzed under vacuum at 110 °C for 26 h in 0.2 ml 6 N HCl-1% phenol. Norleucine was used as an internal standard. Calibration mixtures were used for quantification of unknowns. All samples were run in triplicate. After hydrolysis, a K_3EDTA extraction buffer was used to transfer samples to an Applied Biosystems 420A derivatizer/analyzer. Pre-column derivitization and ion exchange chromatography were used to label and detect free amino acids. Samples were quantitated using Rainin Dynamix data analysis and Microsoft Excel software.

Native Gel Analysis—For stoichiometric titration of 15E8 and other Fab fragments against gp140 by native gel analysis, Fab fragments were titrated against constant amounts of gp140 in various ratios from 1:1 to 1:5 (mol:mol), respectively. Each mixture was incubated overnight at 4 °C and subsequently analyzed on gradient (4–15%) native Phastgel using Phastsystem (Amersham Pharmacia Biotech). The individual components and the complex were visualized by Coomassie Blue staining. The protein concentration of each of the two component mixtures ranged from 4.8 to 13.6 mg/ml.

Immunoprecipitation of gp140-CD4 Complexes by OKT4—To independently assess valency of CD4 binding to gp140, purified gp140 (400 μg) was incubated with s2CD4 and s4CD4 at various concentrations overnight at 4 °C. The molar ratio between gp140 and CD4 was maintained at 1:20. The gp140-CD4 complexes were purified on a Superdex 200 column equilibrated with PBS to remove unbound CD4 at 4 °C. The purified gp140-CD4 complexes were then divided into two aliquots and incubated with either anti-s4CD4-specific mAb OKT4 or KK41 anti-envelope mAb (20 μl of packed Sepharose beads coupled at 5 mg/ml of mAb) for 2 h at 4 °C. Beads were washed five times with PBS including 0.1% Triton X-100 and analyzed on 12% SDS-PAGE.

Analytical Ultracentrifugation—Sedimentation equilibrium experiments were performed using a Beckman XL-A analytical ultracentrifuge equipped with scanning absorbance optics for recording the protein distribution. Three samples (each of 80 μl volume, giving a sample column height of 1.5–2 mm) were loaded into six-channel Yphantis-type centerpieces with their corresponding buffer blanks (10 mM Tris HCl, pH 8.0; 100 μl volume). The An 60 Ti rotor used can accommodate three cell assemblies, thus nine samples were examined during each analytical ultracentrifuge run. Thermodynamic equilibrium was attained at rotor speeds of 20,000 and 24,000 rpm for CD4 and 6,000 rpm for gp140 and the CD4-gp140 mixtures. Equilibrium was ascertained by the satisfactory overlay and subtraction of data acquired 3 h apart. A true optical baseline free from macromolecular species was then obtained by increasing the rotor speed to 40,000 or 47,000 rpm and recording a scan after several hours.

The equilibrium data consist simply of the absorbance measured at the selected scanning wavelength (in this case 282 nm for CD4 and 280 nm for gp140 and the CD4-gp140 mixtures) as a function of the radial

position in the sample column. If the macromolecular system is considered to comprise self-interacting species the concentration at any radial position in the sample column ($c_{total}(r)$) is given by Equation 1 (34),

$$c_{total}(r) = \delta c + \sum_{i=1}^{n} K_{1,i}(C_{1,0}\exp\Big[\sigma\{\xi - \xi_0\} - 2B \sum_{i=1}^{n} C_i(r)\Big])^{q(i)} \quad \text{(Eq. 1)}$$

where δc is proportional to the baseline absorbance; n is the total number of species present in the self-association equilibrium; $K_{1,i}$ is the equilibrium constant for the association of monomer to q(i)-mer; $C_{1,0}$ is the monomer concentration at the radial position of the first data point; σ is the reduced molecular weight ($(M\omega^2(1-\bar{\nu}\rho)/RT$ where M is the monomer mass; ω is the rotor speed in radian/s; $\bar{\nu}$ is the partial specific volume of the protein (ml/g); ρ is the solvent density (g/ml); R is the gas constant (8.31432×10^7 erg/mol K); T is the absolute temperature (K)); ξ and ξ_0 are the values of $r^2/2$ at any point r in the sample column and at the radial position of the first data point respectively; B is the second virial coefficient (here with units of inverse concentration); $C_i(r)$ is the concentration of the i^{th} species at radial position r; q(i) is the degree of association for the i^{th} species. The second virial coefficient describes the reduction in observed mass due to excluded volume and charge repulsion effects. For globular proteins with negligible net surface charge in a solvent of finite salt concentration this term should be minimal.

The value of $\bar{\nu}$ for CD4 and gp140 was estimated from their known amino acid sequences together with a contribution for glycosylation, assuming that all potential glycosylation sites are fully occupied. This gave $\bar{\nu} = 0.738$ ml/g for CD4 and 0.700 ml/g for gp140. Regardless of the ratio of mixtures (3:1, 2:1, or 1:1 in terms of monomers of CD4 per gp140 trimer) the weight average $\bar{\nu}$ of the system was calculated to be 0.710 ml/g. The method of Cohn and Edsall (35) and the consensus partial specific volumes for the constituent amino acids reported by Perkins (36) were used for the $\bar{\nu}$ calculations. The buffer density was calculated (1.0009 g/ml) using the freeware program SEDNTERP (alpha.bbri.org/rasmb/spin/ms_dos/sednterp-philo) (37). Equilibrium solute distribution data were analyzed with the Beckman XL-A data analysis software, which uses a modified form of Equation 1.

RESULTS

SIV Envelope-Human CD4 Interaction—SIVmac32H gp140 envelope was produced in Lec3.2.8.1 cells using a glutamine synthetase recombinant expression system. The latter Chinese hamster ovary cell derivative secretes proteins with homogeneous *N*-linked glycan adducts ($GlcNac_2$-Man_5) but lacking *O*-linked glycans. To prevent any dissociation of the gp120 from the gp41 moiety, both primary and secondary protease cleavage sites were eliminated by mutation of Arg-512 and Lys-523 to glutamic acid residues. In so doing, the heterogeneity of SIV protein could be minimized and the complexity of subsequent analysis reduced as shown below. Additionally, variants of the cleavage site-deficient gp140 precursor protein lacking V1 and V2 loops (ΔV1V2) or V1, V2, and V3 loops (ΔV1V2V3) were produced (28), as well as free gp120.

Fig. 1*A* represents a Superdex 200 gel filtration chromatogram of recombinant SIV envelope previously purified from supernatants of Lec3.2.8.1 gp140 transfectants using a combination of 17A11 anti-SIV mAb affinity purification and gel filtration. As shown, the trimeric SIV gp140 has an apparent molecular mass of ~440 kDa with Ve = 10.32 ml. By 10% SDS-PAGE analysis, a monomer band of ~120 kDa is observed for gp140 with slightly lower molecular masses of 103, 94, and 103 kDa for ΔV1V2, ΔV1V2V3, and gp120, respectively (Fig. 1*A, inset*). In contrast to the SIV gp140 precursor protein, in which the cleavage sites have been eliminated, SIV gp140 protein containing a single intact cleavage site at Lys-523 (C1) chromatographs as three peaks including aggregate, trimeric, and monomeric components while SIV gp140 with both cleavage sites present (C2) is mostly a gp120 monomer by gel filtration (Fig. 1*A*, *right panel margin*).

Fig. 1*B* demonstrates that Lec3.2.8.1 cell-produced s4CD4 comprising amino acids 1–371 has a Ve = 14.42 ml, consistent with the molecular mass of ~45 kDa observed under non-

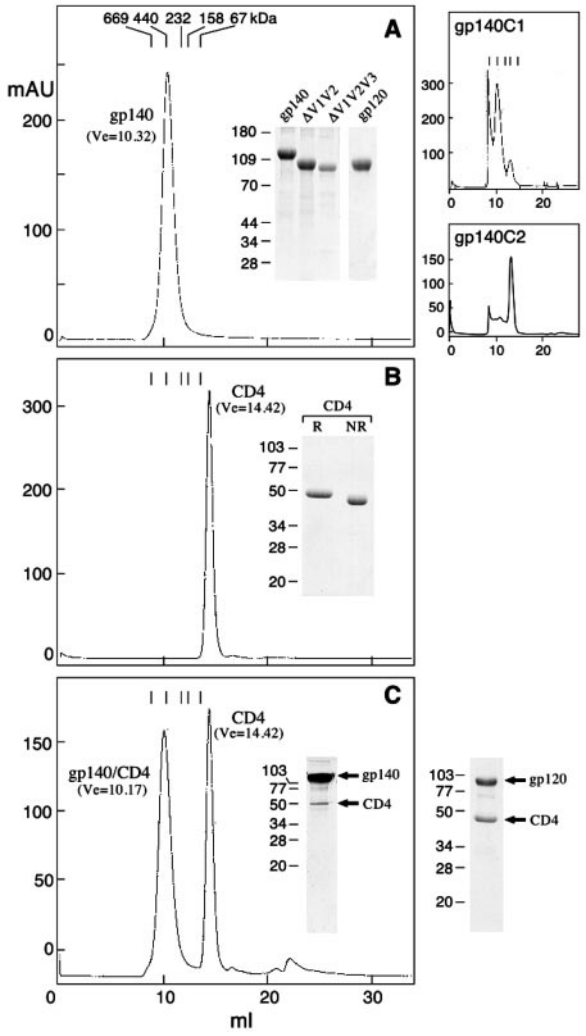

FIG. 1. **Gel filtration chromatography and SDS-PAGE analysis of mac32H SIV gp140 and gp120 proteins and s4CD4.** *A*, the SIV gp140 glycoprotein purified by successive mAb 17A11 affinity chromatography and gel filtration was analyzed on a Superdex 200 HR-30 column. Purified gp140, gp140ΔV1V2, gp140ΔV1V2V3, and gp120 proteins were examined by 10% SDS-PAGE under reducing conditions (*inset*). Superdex 200 chromatography of gp140 C1 and gp140 C2 proteins are shown in the *right margin*. *B,* purified hs4CD4 protein derived from Chinese hamster ovary cells was resized by Superdex 200 chromatography and analyzed by 12% SDS-PAGE under reducing (*R*) or non-reducing (*NR*) conditions. *C,* purified gp140 was incubated with a 30-fold molar excess of s4CD4 overnight at 4 °C and then purified by Superdex 200 chromatography. Peak fractions of the s4CD4-gp140 complex were pooled and analyzed by 15% SDS-PAGE under reducing conditions (*inset*) and compared with a s4CD4-gp120 complex formed using a 5-fold molar s4CD4 excess (*right margin*). All SDS-PAGE gels were stained with Coomassie Blue.

reducing conditions in 12% SDS-PAGE. Note the slightly slower mobility of the s4CD4 extracellular segment under reducing relative to non-reducing conditions, consistent with disruption of intradomain disulfide bonds contributing to a less compact structure. Fig. 1*C* shows that in the presence of a 30-fold molar excess of s4CD4, a complex of gp140-CD4 is formed. This complexed envelope chromatographs slightly differently from uncomplexed gp140 (Ve = 10.17 ml *versus* Ve = 10.32 ml). 15% SDS-PAGE analysis of the complex followed by Coomassie Blue staining (Fig. 1*C, inset*) indicates that the intensity of the gp140 band is much greater than that of the s4CD4 band, suggesting that the stoichiometry of s4CD4 binding to a given SIV trimer may not be 3:1 as predicted (27). In contrast, comparable analysis of the monomeric SIV gp120-

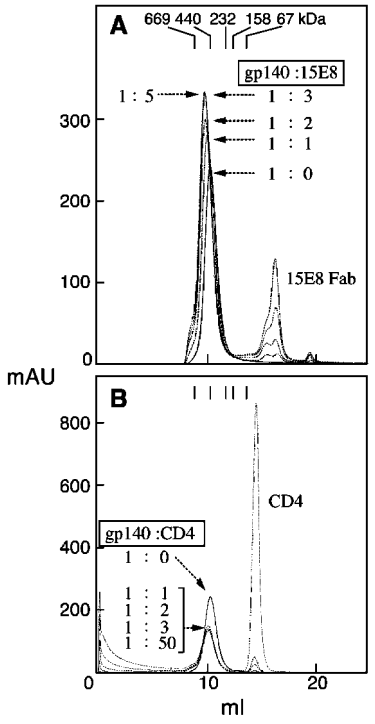

FIG. 2. **Stoichiometry of gp140 complex formation with s4CD4 and 15E8 anti-gp140 Fab proteins.** *A,* purified gp140 protein (200 μg) was mixed with 15E8 Fab fragments in varying ratios ranging from 1:1 to 1:5 (mol:mol). *B,* purified gp140 (100 μg) was mixed with s4CD4 in ratios ranging from 1:1 to 1:50 (mol:mol). Each of the above mixtures was incubated overnight at 4 °C and subsequently analyzed by gel filtration. Note that the gp140 alone (gp140:CD4 = 1:0) represents 200 μg.

CD4 complex shows the two components to be equivalently stained (Fig. 1*C*, *right panel margin*). The chromatographic behavior of the gp140-CD4 complex observed in Fig. 1*C* was obtained with PBS as well as with 20 mM Tris, pH 8. In the experiments, binding and column buffers were identical.

Binding Stoichiometry of s4CD4 and Anti-SIV gp140 Fabs to SIV-gp140 Trimers—To examine more rigorously the binding stoichiometry of CD4 and mAb anti-envelope Fab fragments to SIV-gp140 trimers, we conducted a set of gel filtration studies. Purified SIV gp140 was mixed at various ratios with s4CD4 or 15E8 Fab fragments employing conditions maximizing complex formation, followed by Superdex 200 column chromatography. As shown in Fig. 2*A*, uncomplexed gp140 chromatographs in the expected position (Ve = 10.32 ml). By contrast, 15E8 premixing with gp140 results in formation of a complex with altered chromatographic behavior relative to the free trimer such that Ve = 10.09, 9.89, and 9.81 ml at 1:1, 1:2, and 1:3 gp140:15E8 ratios. Beyond the 1:3 ratio, Fab binding to gp140 is fully saturated. Hence, Ve at 1:3 and Ve at 1:5 are identical. Note that at the highest concentration of 15E8, a readily detectable peak of free Fab (Ve = 16.25 ml) is evident. The small but detectable amount of uncomplexed 15E8 Fab at lower ratios of Fab to gp140 protein may be a consequence of dissociation of the Fab during the chromatography run, may indicate that a fraction of the Fab is unable to bind to gp140, or may result from minor inaccuracy of protein concentration determination. Analysis of 15E8 Fab binding to recombinant trimeric envelope using a native gel mobility shift assay demonstrates enlargement of the complex size as the ratio of gp140 to Fab is changed from 1:1 to 1:2 to 1:3 with discernable excess Fab evident in the Coomassie-stained gel at a greater than 1:3 gp140:15E8 ratio (data not shown). Thus, for the 15E8 Fab, there is an equivalent binding epitope on the three protomers of one SIV gp140 trimer. Consequently, the molar ratio of Fab: trimeric envelope at saturation is 3:1.

The chromatographic behavior of the gp140-CD4 complex is very different (Fig. 2*B*). At a 1:1 molar ratio of gp140 to CD4, the trimer mobility shifts to Ve = 10.17 ml relative to free gp140. However, unlike with the Fab fragments, at gp140:CD4 ratios of 1:2 to 1:50 there is no increase in the relative molecular weight of the formed complex, implying that only one s4CD4 molecule is able to bind to trimeric gp140 in solution. The sample of trimeric gp140 SIV envelope precursor contains no free gp120; thus, the result is not due to shed envelope monomer. Gel shift assays were also consistent with a 1:1 gp140:CD4 stoichiometry (data not shown).

Quantitative Amino Acid Analysis of CD4-SIV gp140 Complexes—To confirm the 1:1 gp140:s4CD4 binding stoichiometry indicated by both molecular sizing chromatography and native gel electrophoresis, quantitative AAA was performed. SIV gp140/s4CD4 protein complexes were generated in the presence of a 30-fold molar excess of s4CD4 and purified by Superdex 200 chromatography. Samples of these complexes as well as purified SIV gp140 alone and purified s4CD4 alone were individually hydrolyzed, and amino acids were quantified. Three independent experimental data sets were obtained, and the average results for leucine and lysine residues are provided in Table I. Although all amino acid residues were analyzed, these two are most informative because the contribution of CD4 in complex is large. For the gp140-CD4 complex, values are given as the average number of residues at 1:1, 1:2, and 1:3 gp140:CD4 ratios in the designated columns as well as the numbers of residues expected by AAA based on the average number of residues of gp140 alone and s4CD4 alone at the indicated stoichiometries. For example, at a 1:1 binding stoichiometry, the quantities of leucine residues in the gp140-CD4 complex should be 163 + 50 = 213. However, based on actual AAA, 199 leucine residues are observed, a 7% variance from the theoretical value. Nonetheless, differences between observed and expected values at 1:2 and 1:3 ratios are larger, 12 and 16%, respectively, consistent with the notion that the 1:1 binding stoichiometry is correct. Similarly, for lysine residues, 140 residues are observed compared with 138 (102 + 36) residues predicted for the complex, a variance of 1%. Of the 17 amino acid residues analyzed, 11 showed the least variance between experimentally observed and expected values for the 1:1 binding stoichiometry. In contrast, only 2–3 residues were found with least variance between observed and expected values at 1:2–1:3 gp140:CD4 ratios. For the 1:3 ratio data, the reliability of the results is questionable given the low number of methionines (five) in s4CD4. Cysteine residues were excluded from consideration in view of the large variance. Collectively, these data argue that the gp140:s4CD4 binding stoichiometry is 1:1. The observed degree of variance between experimental and predicted values is reasonable given potential incompleteness of sample hydrolysis especially in view of the extensive glycosylation of the gp140 moiety. Equivalent analysis utilizing the two-domain s2CD4 *E. coli* protein also demonstrated a 1:1 binding ratio (Table I).

Evidence by Analytical Ultracentrifugation for a 1:1 Binding Ratio of CD4 to gp140—Sedimentation equilibrium yielded information on the stoichiometry of CD4 binding to trimeric gp140 from determination of molecular masses of gp140-CD4 complexes that are independent of shape. The experiments were performed using a Beckman XL-A analytical ultracentrifuge equipped with scanning absorbance optics for recording the protein distribution. All data sets were initially fitted with a model describing a single, thermodynamically ideal macromolecular solute species. In this way an estimate for the ap-

TABLE I
Amino acid analysis of the CD4/gp140 complex indicates a 1:1 binding stoichiometry

Residues	Average number of residues[a]		Average number of residues/residues expected by AAA[b] (% variance gp140-CD4 complex)		
	gp140 alone	CD4 alone	1:1[c]	1:2[c]	1:3[c]
gp140-s4CD4					
Leu	163	50	199/213/(7%)[d]	230/263/(12%)	262/313/(16%)
Lys	102	36	140/138/(1%)	162/174/(7%)	184/210/(12%)
gp140-s2CD4					
Leu	153	20	163/173/(5.7%)	177/193/(8.3%)	191/213/(10.3%)
Lys	106	18	125/124/(0.8%)	136/142/(4.4%)	146/160/(8.4%)

[a] Values of average calculated residues are based on three independent experimental data sets with mean values given. Standard deviations for gp140 and CD4 residues were 0–8% and 3–8% for leu and lys, respectively.
[b] Values of residues expected by AAA are based on theoretical valency of binding (1:1, 1:2, or 1:3) using the avg. cal. res. from AAA determination.
[c] gp140-CD4 ratio.
[d] Numbers in parentheses represent variance between experimentally derived and theoretical values such that % variance = expected residues − calculated residues/expected residues.

parent whole-cell weight average molecular mass ($M_{w,app}$) was obtained for each loading concentration of s4CD4, gp140, or the mixture. These reduced data are plotted as a function of monomer-loading concentration for s4CD4 and gp140 in Fig. 3. $M_{w,app}$ does not vary greatly with CD4 concentration nor with rotor speed. Extrapolation of the two data sets to infinite dilution yields masses of 46.2 ± 1.4 kDa and 44.0 ± 0.8 kDa from the 20,000 rpm and 24,000 rpm data, respectively (Fig. 3*A*). Comparison of these values with the calculated monomer mass for CD4 (43,942 Da) implies that CD4 is a monomer at the concentrations studied. In addition to this, the solute distributions were well fit with the form of Equation 1 (see "Experimental Procedures") describing a thermodynamically ideal monomeric solute. The fits of the simplest form of the equation to the solute distributions for gp140 were not as good as those obtained for CD4; there was evidence for the presence of a higher mass species near the base of the solute column. In Fig. 3*B*, $M_{w,app}$ is plotted as a function of trimer concentration for gp140; extrapolation of these reduced data to infinite dilution gives M^0 = 395.6 ± 14.8 kDa. Trimeric gp140 would have a mass of 331,350 Da (assuming full occupancy of the glycosylation sites). Thus, M^0 implies the presence of a higher oligomer (or aggregate). It was possible to obtain a marginal improvement to some of the fits to the raw data using the form of Equation 1, which describes a self-associating system, in particular a monomer-dimer system. In the case of gp140 "monomer", this is in fact a trimer-hexamer equilibrium. The dissociation constants so obtained were small, averaging at 2.3 μM (on the gp140 trimer concentration scale). Thus, at the concentrations used in these studies, gp140 is mostly trimeric in solution with the presence of a small amount of hexamer or a small amount of aggregate.

Assuming that gp140 is largely trimeric, mixtures of s4CD4 and gp140 were prepared to examine three possible stoichiometries of interaction: 3:1, 2:1, and 1:1 (s4CD4 monomer:gp140 trimer). Not surprisingly, suboptimal fits were obtained when the thermodynamically ideal monomeric solute form of Equation 1 was used to fit the solute distributions acquired for these mixtures. The values of $M_{w,app}$ are, however, plotted as a function of s4CD4:gp140 stoichiometry in Fig. 3*C*. As shown, there is little dependence of $M_{w,app}$ upon total protein concentration but very strong dependence on the stoichiometry of the mixture.

To interpret the data summarized in Fig. 3*C* the whole-cell weight-average mass was calculated for the three stoichiometry mixtures used depending on the mode of binding. This calculation was made more complex by the possibility of gp140 existing in a trimer-hexamer equilibrium. However, the data in Table II reveal that, irrespective of this possibility, the conclusions remain the same. Across the table, the 1:1 association model agrees most closely with the experimentally determined values for $M_{w,app}$. Thus, according to sedimentation equilibrium studies, the mode of association between s4CD4 and gp140 is 1 CD4 monomer per gp140 trimer.

Envelope Binding Competition Using s4CD4 and s2CD4 Proteins and OKT4—It has been suggested that multimeric CD4 binding by HIV envelope protein oligomers is required for gp120 dissociation as well as for viral adsorption and penetration (38, 39). In this regard, Earl *et al.* (40) previously presented data in favor of multimeric CD4 binding exhibited by cell surface envelope proteins using an OKT4 coprecipitation assay. To determine stoichiometry of CD4 binding, we adopted this coprecipitation assay but using the purified soluble trimeric SIVmac32H gp140 precursor instead of detergent-soluble envelope-expressing cell lysates. OKT4 recognizes s4CD4 but not s2CD4. Thus, if trimeric gp140 proteins were incubated with equimolar amounts of s4CD4 and s2CD4, OKT4 would coprecipitate s2CD4 and gp140 in the case of multimeric CD4 binding to an envelope trimer. In contrast, neither free s2CD4 nor s2CD4 bound to gp140 should be immunoprecipitated under these conditions if a single CD4 molecule binds to one gp140 trimer. For this experiment, purified gp140 proteins were incubated with s2CD4 and s4CD4 in various concentrations at 4 °C overnight. CD4-gp140 complexes were subsequently purified by Superdex 75 column to remove unbound CD4. The purified CD4-gp140 complexes were then divided into two aliquots and immunoprecipitated with either the anti-gp140 KK41 mAb or the anti-CD4 OKT4 mAb. As shown in Fig. 4, the amount of s4CD4 coprecipitated by anti-gp140 at various s4CD4 concentrations was identical to the amount of s4CD4 immunoprecipitated by OKT4, indicating that only gp140-bound s4CD4 remains after gel filtration and that little, if any, dissociation of s4CD4 from gp140 occurs during immunoprecipitation. Furthermore, when gp140 proteins are incubated with s4CD4 and s2CD4, anti-gp140 coprecipitates both s4CD4 and s2CD4 proteins (Fig. 4*A*) with a predictable stoichiometry based on ratios of the input s4CD4 and s2CD4 proteins. On the other hand, in contrast to anti-gp140, the OKT4 mAb immunoprecipitated only s4CD4, demonstrating that one CD4 molecule binds to each trimeric gp140. Our result is not in agreement with multimeric CD4 binding observed by Earl *et al.* (40). Possible explanations for this discrepancy may be that aggregation of trimeric transmembrane envelope proteins during cell lysis could result in coprecipitation of s2CD4 bound to one envelope protein and s4CD4 bound to another envelope protein molecule. Alternatively, nonspecific binding of gp140 to OKT4 may play a role in coprecipitation of s2CD4 bound to gp140 (Fig. 4*B*). Specific SIV and HIV trimers may also differ with respect to anti-cooperativity observed (see below).

Kinetic Analysis of the s4CD4-gp140 and s4CD4-gp120 In-

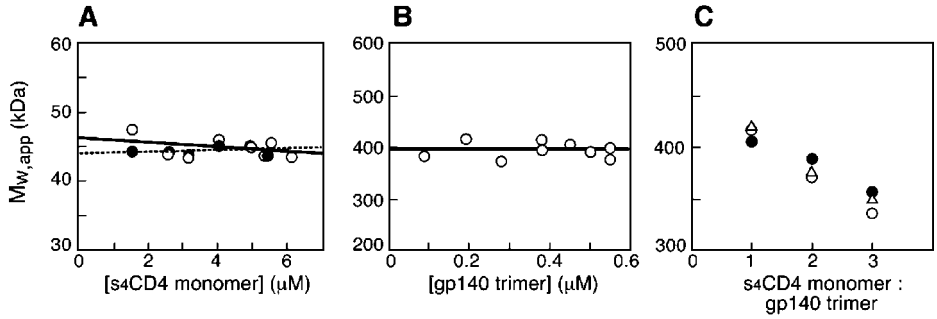

FIG. 3. **Sedimentation equilibrium analysis of gp140/s4CD4 complexes.** *A,* apparent whole cell weight average molecular mass plotted as a function of monomer loading concentration for CD4. Data were acquired at rotor speeds of 20,000 rpm (○) and 24,000 rpm (●). *B,* apparent whole cell weight average apparent molecular mass plotted as a function of trimer-loading concentration for gp140. *C*), apparent whole cell weight average apparent molecular mass plotted as a function of the stoichiometry of the CD4-gp140 mixture (as a molar ratio) for three different total loading concentrations (0.5 μM (○), 1.0 μM (△) and 1.5 μM (●) CD4).

TABLE II
Comparison of experimentally determined apparent whole cell weight average molecular mass with that calculated for different models of association of CD4 with gp140 trimer

Model	Trimer-hexamer equilibrium	$M_{w,app}$		
		1:1[a]	2:1[a]	3:1[a]
Experimental $M_{w,app}$ (kDa)[b]		413 ± 7	378 ± 9	346 ± 10
No association between CD4 and gp140	No $(gp140)_6$[c]	347	310	281
	+ $(gp140)_6$[d]	372	334	305
1:1 association ($CD4:(gp140)_3$)	No $(gp140)_6$	441	394	356
	+ $(gp140)_6$	432	388	353
3:1 association ($CD4_3:(gp140)_3$)	No $(gp140)_6$	454	499	534
	+ $(gp140)_6$	456	495	475

[a] Stoichiometry ($CD4:gp140_3$).
[b] The average of the three data obtained with the three different total loading concentrations for each stoichiometric mixture.
[c] For this calculation, the presence of aggregate or hexameric gp140 was ignored and all gp140 was presumed to be in trimeric form.
[d] For this calculation, gp140 was presumed to exist in a trimer-hexamer equilibrium with K_a = 2.32 μM.

teraction—Surface plasmon resonance was used to examine the kinetics of the trimeric gp140-CD4 interaction and was compared with that of monomeric gp120-CD4. To determine the binding kinetics of trimeric gp140 to CD4, s4CD4 was immobilized and gp140 protein passed over the chip surface in increasing molar amounts. Representative kinetic data are shown as sensorgrams in Fig. 5*A*. Data were fitted to a 1:1 binding model over the entire injection period. Kinetic data are summarized for two independent experiments in Fig. 5*C*. The K_d for gp140-CD4 interaction calculated from the ratio of k_{off}:k_{on} ranges from 190–210 nM. A relatively slow k_{on} is evident ($4.4–4.6 \times 10^3$ M^{-1} s^{-1}). Fig. 5*B* shows data for monomeric gp120 on the sCD4 surface. While the k_{on} is similar, the k_{off} is 3- to 4-fold slower, resulting in a longer $t_{1/2}$ and a K_d ~60 nM (Fig. 5*C*). This K_d value lies between previously reported values of 0.2–0.4 nM for the gp120 from SIVagm TYO-7 and 82–350 nM for gp120 of SIVmac (41–43). Consistent with these data, trimer-expressing virions of primary HIV-1 isolates have shown resistance to soluble CD4 with lower affinity for CD4 binding than that of recombinant monomeric gp120 (21).

Characterization of Anti-SIV Envelope mAbs That Neutralize Viral Infection—Prior studies have suggested that viral neutralization by an antibody is a function of its binding kinetics, valency, epitope specificity, and/or binding site localization (44–47). To investigate SIV neutralization, we utilized four mAbs generated against virion-derived envelope as well as nine mAbs generated against SIV mac32H gp140 protein. As shown in Table III, of the mAbs tested, four (KK9, 17A11, 2C3, and 2C9) are potent at neutralizing the SIV mac251 strain (ID_{50} <1 μg/ml), one (9G3) is weakly neutralizing (ID_{50} = 9.51 μg/ml), and the remaining nine mAbs are without detectable activity (ID_{50} >50 μg/ml). None of these mAbs cross-neutralize the unrelated SIV strains 239, smH-4, or deltaB670. Mapping studies, assessment of an epitope's conformational *versus* linear character, kinetic antibody binding parameters, and valency of interaction were examined.

Each of the mAbs whose Fab fragments were generated and purified showed a stoichiometry of binding to the trimeric gp140 envelope of 3:1 (Fig. 2 and data not shown). Hence, valency *per se* is not a determinant of neutralization. As shown in Table III, epitope mapping studies clearly localize a major neutralizing epitope site: KK9, 17A11, 2C3, and 2C9 map to the V3V4 region and cross-block each other's binding. Among the four mAbs, KK9 is most dependent on the V3 loop. Furthermore, none of the epitopes identified by these neutralizing mAbs is detected in Western blots of denatured and reduced gp140, implying that these mAbs, unlike the other nine mAbs, recognize native conformational determinants (Table III and data not shown). In contrast, the non-neutralizing 10B11 mAb, which partially cross-blocks KK9 and localizes nearby to the V3 loop, identifies its epitope in Western blot analysis.

Kinetic analysis of mAb binding to trimeric gp140 shows that k_{on} varies from 3.5×10^4 to 9.3×10^6 M^{-1} s^{-1} with k_{off} from $1.3–5.9 \times 10^{-3}$ s^{-1}. Thus, the greatest determinant of affinity is the k_{on}, which varies by 200- to 300-fold for those mAbs. While each of the four strongly neutralizing mAbs has a K_d = 2.3–4.1 nM, affinity as such is not the only determinant of neutralization. The gp41-specific KK41 mAb, for example, possesses a K_d = 2.1 nM with the fastest k_{on} of the antibodies tested (9.3×10^6 M^{-1} s^{-1}) but is non-neutralizing. Additional evidence comes from analysis of 9G3. This mAb, like KK41, binds to gp41 and is partially overlapping with KK41 as shown by cross-blocking studies. Nonetheless, 9G3 has neutralizing activity whereas KK41 is non-neutralizing even though 9G3

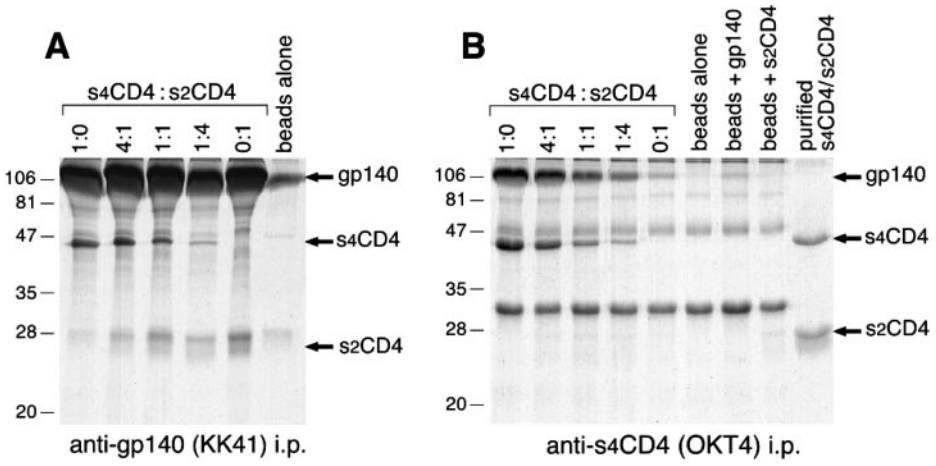

FIG. 4. **Evidence for binding of a single CD4 molecule to trimeric gp140 by biochemical analysis.** Trimeric gp140 was incubated with s4CD4 and s2CD4 at various concentrations at 4 °C overnight, maintaining a 1:20 molar ratio between gp140 and CD4. The gp140-CD4 complexes were subsequently purified on a Superdex 200 column to remove unbound CD4. Equivalent amounts of gp140-CD4 complexes were then incubated with either anti-gp140 antibody KK41 (*A*) or anti-s4CD4-specific antibody OKT4 (*B*) and analyzed on 12% SDS-PAGE stained with Coomassie Blue.

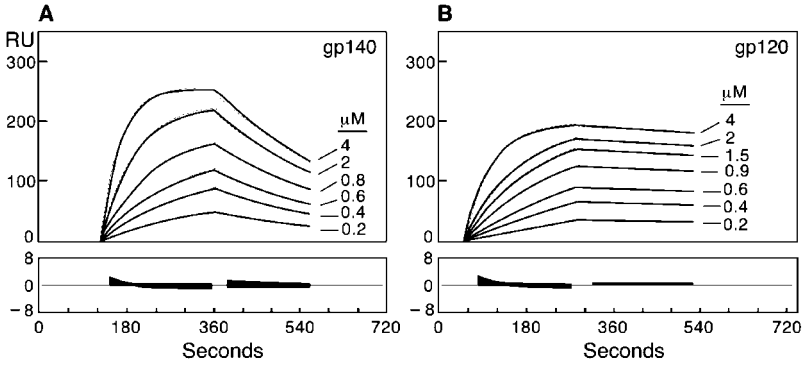

C

Analyte/Ligand		k_{on} ($M^{-1}•S^{-1}$)	k_{off} (S^{-1})	$t_{1/2}$ (S)	K_D (nM)
gp140/s4CD4	1	4.6×10^3	9.9×10^{-4}	700	210
	2	4.4×10^3	8.6×10^{-4}	805	190
gp120/s4CD4	1	4.5×10^3	2.3×10^{-4}	3013	52
	2	4.2×10^3	3.0×10^{-4}	2310	71

FIG. 5. **Sensorgram overlays for gp140 (*A*) and gp120 (*B*) binding to an s4CD4 surface.** *Thin lines* are fit to a 1:1 binding model. *Solid lines* represent experimental data. Concentrations of gp140 and gp120 analytes injected over the s4CD4 surface are indicated. Residuals are plotted *below* the sensorgrams. *C,* summary of the kinetics of the s4CD4 interaction with gp140 and gp120 proteins.

affinity is slightly weaker than that of KK41 (K_d = 3.7 *versus* 2.1 nM). Preincubation of gp140 with s4CD4 prior to mAb binding, as described under "Experimental Procedures", does not alter the K_d of any of the mAbs by more than a factor of 2, indicating that none of the mAbs recognizes an envelope epitope whose conformation is affected in a major way by CD4 ligation. This does not exclude the possibility that such antibodies exist, however.

DISCUSSION

Our finding that only one CD4 molecule can readily bind to an SIV envelope trimer is unexpected. Nonetheless, this conclusion results from independent evaluations of gp140-CD4 complexes using molecular sizing chromatography, gel mobility shift assays, quantitative amino acid analysis, and analytical ultracentrifugation. Steric blockage of the two other potential CD4 binding sites on a trimer by s4CD4 itself is an unlikely explanation of the results because s2CD4, a truncated D1D2 envelope-binding fragment of CD4, also has the same binding characteristics (Table I). How then can the observed stoichiometry be rationalized?

The Fab binding analyses show that the trimer itself must be a symmetric structure. None of the monoclonals in our panel, which recognize epitopes distributed widely across the surface of the molecule, appears to exhibit interference between related sites on a trimer. By contrast, when CD4 binds, a striking asymmetry is induced that effectively blocks the other two sites. One potential source of this asymmetry is the constraint imposed on the molecule by the intact cleavage site between gp120 and gp41. When CD4 binds to one subunit in a trimer, it induces a conformational change that transforms the target gp120 into a conformation probably very close to the one seen in the CD4/Fab/gp120-core complex studied by Kwong *et al.* (26). If this change included displacements possible only if the C terminus of gp120 and the N terminus of gp41 could move relative to one another, then the changes induced in the uncleaved trimer would be incomplete and the trimer might accommodate CD4 ligation by adopting an asymmetric structure. The asymmetry would prevent the other subunits from undergoing a similar transition and thus would strongly reduce their effective affinity for CD4.

An alternative hypothesis is that CD4 binding induces asymmetry even in a cleaved gp140 trimer. CD4 binding to one gp120 on a trimer clearly produces strain, since the affinity of CD4 for gp120 on trimers is generally lower than its affinity for free gp120 from the same viral isolate. The trimer adapts to this imposed strain by shifting to a conformation that reveals a co-receptor binding site but that is inherently less stable than the "ground state". Based on the kinetic analysis here, the conformational adaptation of one gp120 subunit in a trimer is not as favorable as of a gp120 monomer, hence yielding a faster CD4 off rate for the former. If the conformational change induced in the first subunit to bind produced sufficient strain in

TABLE III
Characteristics of neutralizing vs. non-neutralizing anti-gp140 mAbs: epitope mapping and kinetics of binding

mAb[a]	Immunogen[b]	Epitope map[c]	Cross-blocking[d]	Western blot[e]	Neutralization[f]	k_{on}[g]	k_{off}[g]	K_d[g]
						$M^{-1}\ s^{-1}$	s^{-1}	nM
KK19	virion	V1V2	10H3	+	>50	7.1×10^4	1.7×10^{-3}	24 (18)
10H3	gp140	V1V2	KK19	+	>50	6.5×10^5	1.4×10^{-3}	21 (17)
KK9	virion	V3	17A11,2C3,2C9	−	0.1–3.1	9.3×10^5	3.8×10^{-3}	4.1 (8.0)
17A11	virion	V3V4	KK9,2C3,2C9	−	0.21	5.6×10^5	1.5×10^{-3}	2.8 (3.7)
2C3	gp140	V3V4	KK9,17A11,2C9	−	0.17	7.2×10^5	1.6×10^{-3}	2.3 (2.5)
2C9	gp140	V3V4	KK9,17A11,2C3	−	0.32	3.9×10^5	1.4×10^{-3}	3.5 (3.2)
10B11	gp140	V3 "plus"	pKK9	+	>50	3.9×10^4	2.2×10^{-3}	56 (32)
13H10	gp140	unknown		+	>50	3.5×10^4	2.0×10^{-3}	59 (75)
15E8	gp140	unknown		+	>50	1.0×10^5	1.9×10^{-3}	19 (14)
116	ΔV1V2V3	unknown		+	>50	2.5×10^5	1.9×10^{-3}	7.7 (8.0)
KK41	virion	gp41	p9G3	+	>50	9.3×10^6	1.9×10^{-3}	2.1 (1.3)
9G3	gp140	gp41	pKK41	+	9.51	3.4×10^5	1.3×10^{-3}	3.7 (5.3)
11D11	gp140	gp41		+	>50	6.9×10^5	5.9×10^{-3}	8.0 (7.7)

[a] mAbs are all of the IgG1 murine isotype.
[b] The immunogens for mAb production include virion related, a combination of recombinant vaccinia virus plus SIV-infected cells for KK19, KK9 and KK41 (66, 67) or SIV-infected cells alone (17A11) or a baculovirus produced mac32H (pJ5) gp140 for all the mAbs except 116 which utilized the baculovirus produced gp140 ΔV1V2V3 variant.
[c] Epitope mapping is based on reactivity binding profile and cross-blocking studies on BIAcore and prior studies (68, 69) mapping KK9 to V3 and V4 regions. V3 "plus" designation for 10B11 is based on incomplete elimination of binding by the ΔV1V2V3 mutation. gp41 specificity is based on reactivity with chimeras ADA gp120-SIV gp41 fusion protein. V1V2 assignment was based on loss of antibody reactivity on ΔV1V2 deleted gp140.
[d] Cross-blocking. Unless indicated, cross-blocking is complete. In the case of 10B11, KK41 and 9G3 cross-blocking is only partial (~50% inhibition), indicated by "p".
[e] For Western blot, "+" indicates that the mAb detects by Western blot gp140 run in SDS-PAGE under reducing conditions whereas "−" indicates no discernable reactivity.
[f] Neutralization assays were performed as described in "Materials and Methods" where values are expressed as ID_{50} (μg/ml). For KK9 0.1–3.1 μg/ml are reported (70). All other values are derived from the experiments herein where antibodies were tested in a minimum of two or more separate experiments.
[g] Kinetics measurements are based on BIAcore data. All numbers in parentheses represent mAb binding to gp140 after the envelope has bound s4CD4.

the neighbors to prevent symmetrical conformational changes and hence, to block their capacity to bind CD4, we might expect high concentrations of CD4 to induce gp120 dissociation (freeing it from the trimeric constraints and allowing it to open up and bind CD4). CD4-induced shedding of gp120 has indeed been described (48), but there are of course additional ways to account for this observation.

Due to dissociation of gp120 from gp41, we have not succeeded in purification of an intact gp120-gp41 complex where the two components are in noncovalent association. Hence, the study of the stoichiometry of CD4 binding comparable with that made with the non-cleavable gp140 precursor could not be conducted. Furthermore, digestion of purified and uncleaved gp140 C1 envelope protein *in vitro* by furin was not able to generate gp120 and gp41 component products (data not shown). Envelope glycosylation may protect the furin cleavage site from digestion or additional enzymes may be required to generate the mature envelope fragments.

Recently, Salzwedel and Berger (49) presented evidence for cooperative subunit interaction within the oligomeric envelope glycoprotein of HIV in the fusion process using a genetic complementation analysis. By examining a series of envelope variants with defects at specific functional sites in either gp120 or gp41 that render the glycoprotein incompetent for fusion with a CD4 target cell bearing a particular co-receptor, they showed that fusion can occur when one gp120 subunit is defective for CD4 binding or for co-receptor binding as long as it can pair with a subunit with intact function. A similar result was shown with complementation of normal and fusion-defective gp41 components. These data are consistent with the notion that binding of a single CD4 molecule to a trimeric envelope protein is sufficient to trigger conformational change in the native oligomer, subsequently followed by co-receptor binding and fusion.

Whatever the detailed mechanism underlying the observed anti-cooperativity of CD4 binding to trimeric gp140, we can conclude that there must be a significant rearrangement in gp120 on the surface of a trimer when it binds CD4, perhaps including reorganization of the polypeptide chain near the gp120/gp41 cleavage point. Binding of the Fabs analyzed here appears not to induce this conformational change since we did not observe comparable anti-cooperativity. In the event that only the binding of a single CD4 molecule to a viral trimeric gp160 spike is necessary to trigger conformational change leading to fusion, antibody-related viral neutralization would be at a distinct disadvantage; blockade by a given antibody of all three sites on the trimer is then required to prevent viral binding and fusion.

Any of a number of theories have been proposed to explain the basis upon which only certain antibodies neutralize viruses. Kinetic parameters including fast on rates and slow off rates have been identified (44, 46). Others have emphasized qualitative differences between neutralizing *versus* non-neutralizing antibodies. For example, anti-envelope antibodies that bind to the envelope spike on the virion will be neutralizing whereas those that bind to viral peptide fragments and/or monomeric envelope components will fail to be neutralizing (50). In the case of HIV1, it has been further suggested that neutralization by antibody is determined primarily by occupancy sites on the virion, regardless of epitope specificity (45).

The present findings speak to these issues in specific molecular terms. Thus, while a threshold affinity is required for neutralization, site-specific localization of epitope binding is critical. For example, although KK41 binds SIV envelope with a K_d = 2.1 nM, equivalent to the neutralizing mAb 2C3 (2.3 nM), the KK41 mAb is not neutralizing. This confirms other observations that certain mAbs and human anti-C4 mAbs bind well to intact virions but do not neutralize the virus (51–53). Moreover, four of the five neutralizing antibodies identified here recognize a native V3V4 conformational epitope as judged by their inability to detectably bind to denatured gp140 in Western blot analysis. These mAbs may directly or indirectly interfere with chemokine receptor binding; such mAbs are known to be neutralizing (30). These findings emphasize the view that

most neutralizing antibodies recognize epitopes that contribute to an accessible functional site on the native trimer structure of the virion. Nevertheless, that non-conformational epitopes may be neutralizing, at least under some circumstances, is evident from the analysis of the gp41-specific 9G3 mAb. Consistent with this finding is the observation that the broadly neutralizing antibody 2F5 recognizes a linear sequence epitope ELDKWA in the membrane proximal segment of HIV1-gp41 (54).

In the current study, we did not generate CD4 binding site-specific mAbs. Kinetic data showed that the affinity of CD4 to a gp140 trimer is weaker than that of CD4 to a gp120 monomer. Perhaps the CD4 binding site is partially occluded by the interactions between gp120 subunits in a trimer, necessitating conformational alterations. The resistance of primary HIV-1 isolates to soluble CD4 therapy has been attributed to a lower binding affinity of primary virus envelope glycoprotein oligomers for CD4 (46, 55, 56). Although anti-CD4 mAb binding site epitopes and the CD4 binding site overlap, mapping studies demonstrate that they are not identical (57). In the crystal structure of the gp120-CD4-Fab complex, a number of the residues contributing to CD4 binding site epitopes are located in a depression at the interface between the inner and outer gp120 domains, a configuration that may offer poor immunogenicity. Furthermore, CD4 binding site antibodies might recognize a native gp120 conformation that is altered in the CD4-bound state (26). Dynamic alterations of the CD4 binding site may foster poor antibody complementarity, resulting in only modest antibody affinity for the site. Occlusion of the CD4 binding site epitopes by CD4 may delay the generation of high affinity antibodies against the CD4 binding site epitopes. Hence, CD4 binding site epitopes alone may not be sufficient targets for vaccine development. Synergy between antibodies directed against CD4 binding site epitopes and other unrelated epitopes have been reported (58–61).

Elicitation of neutralizing antibodies by oligomeric forms of soluble gp140 has been disappointing to date, perhaps because those tested oligomers are mostly dimers or tetramers and modified trimers (62–64). Nonetheless, recent comparison of antibody responses in rabbits to HIV gp120 and gp140 produced and purified in an identical manner showed that gp140 elicits enhanced cross-reactivity with heterologous envelope proteins as well as greater neutralization (65). Trimeric uncleaved gp140 produced as described here seems to be a physiologic representation of the native envelope structure on the virus particle and may offer a prototype for a useful immunogen. The structure of the trimeric envelope glycoprotein in its non-CD4 contacted ground state might provide the needed clues for rational design of a protein fragment capable of eliciting neutralizing antibodies to the native molecule.

Acknowledgments—We thank our colleagues Drs. Yi Xiong for providing s4CD4 containing Lec3.2.8.1 supernatants, Margaret Pietras for assisting with mAb production, and Jim Lee and Angelo Dickerson for AAA. We thank Dr. Robert W. Doms for assessing the chemokine receptor binding activity of the trimeric envelope and Karen Kent for providing the mAbs.

REFERENCES

1. Barre-Sinoussi, F., Chermann, J. C., Rey, F., Nugeyre, M. T., Chamaret, S., Gruest, J., Dauget, C., Axler-Bin, C., Vezinet-Brun, F., Rouzioux, C., Rozenbaum, W., and Montagnier, L. (1983) *Science* **220,** 868–871
2. Gallo, R. C., Salahuddin, S. Z., Popovic, M., Shearer, G. M., Kaplan, M., Haynes, B. F., Palker, T. J., Redfield, R., Oleske, J., Safai, B., White, G., Foster, P., and Markham, P. D. (1984) *Science* **224,** 500–503
3. Letvin, N. L., Daniel, M. D., Sehgal, P. K., Desrosiers, R. C., Hunt, R. D., Waldron, L. M., MacKey, J. J., Schmidt, D. K., Chalifoux, L. V., and King, N. W. (1985) *Science* **230,** 71–73
4. Daniel, M. D., Letvin, N. L., King, N. W., Kannagi, M., Sehgal, P. K., Hunt, R. D., Kanki, P. J., Essex, M., and Desrosiers, R. C. (1985) *Science* **228,** 1201–1204
5. Murphey-Corb, M., Martin, L. N., Rangan, S. R. S., Baskin, G. B., Gormus, B. J., Wolf, R. H., Ades, W. A., West, M., and Montelaro, R. C. (1986) *Nature* **321,** 435–437
6. Benveniste, R. E., Morton, W. R., Clark, E. A., Tsai, C. C., Ochs, H. D., Ward, J. M., Kuller, L., Knott, W. B., Hill, R. W., and Gale, M. J. (1988) *J. Virol.* **62,** 2091–2101
7. Desrosiers, R. C. (1988) *Ann. Rev. Microbiol.* **42,** 607–625
8. Klatzmann, D., Barre-Sinoussi, F., Nugeyre, M. T., Danquet, C., Vilmer, E., Griscelli, C., Brun-Veziret, F., Rouzioux, C., Gluckman, J. C., Chermann, J. C., *et al*. (1984) *Science* **225,** 59–63
9. Dalgleish, A. G., Beverley, P. C., Clapham, P. R., Crawford, D. H., Greaves, M. F., and Weiss, R. A. (1984) *Nature* **312,** 763–767
10. Sattentau, Q., Dalgleish, A., Weiss, R., and Beverley, P. C. L. (1986) *Science* **234,** 1120–1123
11. McDougal, J. S., Nicholson, J. K., Cross, G. D., Cort, S. P., Kennedy, M. S., and Mawle, A. C. (1986) *J. Immunol.* **137,** 2937–2944
12. McDougal, J. S., Kennedy, M. S., Slight, J. M., Cort, S. P., Mawle, A. C., and Nicholson, J. K. (1986) *Science* **231,** 382–385
13. Maddon, P., Dalgleish, A., McDougal, J. S., Clapham, P. R., Weiss, R. A., and Axel, R. (1986) *Cell* **47,** 333–348
14. Robey, W. G., Safai, B., Oroszlan, S., Arthur, L. Q., Gonda, M. A., Gallo, R. C., and Fischinger, P. J. (1985) *Science* **228,** 593–595
15. Veronese, F. D., DeVico, A. L., Copeland, T. D., Oroszlan, S., Gallo, R. S., and Sarngadharan, M. G. (1985) *Science* **229,** 1402–1405
16. Sattentau, Q. J., and Moore, J. P. (1991) *J. Exp. Med.* **174,** 407–415
17. Sattentau, Q. J., Moore, J. P., Vignaux, F., Traincard, F., and Poignard, P. (1993) *J. Virol.* **67,** 7383–7393
18. Furuta, R. A., Wild, C. T., Weng, Y., and Weiss, C. D. (1998) *Nat. Struct. Biol.* **5,** 276–279
19. Feng, Y., Broder, C. C., Kennedy, P. E., and Berger, E. A. (1996) *Science* **272,** 872–877
20. Alkhatib, G., Combadiere, C., Broder, C. C., Feng, Y., Kennedy, P. E., Murphy, P. M., and Berger, E. A. (1996) *Science* **272,** 1955–1958
21. Moore, J. P., McKeating, J. A., Huang, Y., Ashkenazi, A., and Ho, D. D. (1992) *J. Virol.* **66,** 235–243
22. Mulligan, M. J., Ritter, G. D., Chailkin, M. A., Yamshchikov, G. V., Kumar, P., Hahn, B. H., Sweet, R. W., and Compans, R. W. (1992) *Virol* **187,** 233–241
23. Weissenhorn, W., Dessen, A., Harrison, S. C., Skehel, J. J., and Wiley, D. C. (1997) *Nature* **387,** 426–430
24. Chan, D. C., Fass, D., Berger, J. M., and Kim, P. S. (1997) *Cell* **89,** 263–273
25. Tan, K., Liu, J., Wang, J., Sehn, S., and Lu, M. (1997) *Proc. Natl. Acad. Sci. U. S. A.* **94,** 12303–12308
26. Kwong, P. D., Wyatt, R., Robinson, J., Sweet, R. W., Sodroski, J., and Hendrickson, W. A. (1998) *Nature* **393,** 648–659
27. Kwong, P. D., Wyatt, R., Sattentau, Q. J., Sodroski, J., and Hendrickson, W. A. (2000) *J. Virol.* **74,** 1961–1972
28. Chen, B., Zhou, G., Kim, M., Chishti, Y., Hussey, R. E., Ely, B., Skehel, J. J., Reinherz, E. L., Harrison, S. C., and Wiley, D. C. (2000) *J. Biol. Chem.* **275,** 34946–34953
29. Liu, J., Tse, A. G. D., Chang, H.-C., Liu, J.-H., Wang, J., Hussey, R. E., Chishti, Y., Rheinhold, B., Spoerl, R., Nathenson, S. G., Sacchettini, J. C., and Reinherz, E. L. (1996) *J. Biol. Chem.* **271,** 33639–33646
30. Edinger, A. L., Ahuja, M., Sung, T., Baxter, K. C., Haggerty, B., Doms, R. W., and Hoxie, J. A. (2000) *J. Virol.* **74,** 7922–7935
31. Xiong, Y., Kern, P., Chang, H.-C., and Reinherz, E. L. (2001) *J. Biol. Chem.* **276,** 5659–5667
32. Wang, J., Yan, Y., Garrett, T. P. J., Liu, J., Rodgers, D. W., Garlick, R. L., Tarr, G. E., Husain, Y., Reinherz, E. L., and Harrison, S. C. (1990) *Nature* **348,** 411–418
33. Langlois, A. J., Desrosiers, R. C., Lewis, M. G., Kewalramani, V. N., Littman, D. R., Zhou, J. Y., Manson, K., Wyand, M. S., Bolognesi, D. P., and Montefiori, D. C. (1998) *J. Virol.* **72,** 6950–6955
34. Kim, H., Deonier, R. C., and Williams, J. W. (1977) *Chem. Rev.* **77,** 659–690
35. Cohn, E. J., and Edsall, J. T. (1943) *Proteins, Amino Acids, and Peptides As Ions and Dipolar Ions.* American Chemical Society Monograph Series, Reinhold Publishing Corp., New York
36. Perkins, S. J. (1986) *Eur. J. Biochem.* **157,** 169–180
37. Laue, T. M., Shah, D. D., Ridgeway, T. M., and Pelletier, S. L. (1992) in *Analytical Ultracentrifugation in Biochemistry and Polymer Science* (Harding, S. E., Rowe, A. J., and Horton, J. C., eds), pp. 90–125, Royal Society of Chemistry, Cambridge, UK
38. Layne, S. P., Merges, M. J., Dembo, M. B., Spouge, J. L., and Nara, P. L. (1990) *Nature* **346,** 277–279
39. Moore, J. P., McKeating, J. A., Norton, W. A., and Sattentau, Q. J. (1991) *J. Virol.* **65,** 1133–1140
40. Earl, P. L., Doms, R. W., and Moss, B. (1992) *J. Virol.* **66,** 5610–5614
41. Jones, D. H., McBride, B. W., Roff, M. A., Maloney, V., and Farrar, G. H. (1994) *Vaccine* **12,** 250–254
42. Matthews, T. J., Weinhold, K. J., Kim Lyerly, H., Langlois, A. J., Wigzell, H., and Bolognesi, D. P. (1987) *Proc. Natl. Acad. Sci. U. S. A.* **84,** 5424–5428
43. Polzein, F., Scharf, J.-G., Luke, W., and Hunsmann, G. (1992) *AIDS Res. Hum. Retroviruses* **8,** 1171–1177
44. VanCott, T. C., Bethke, F. R., Polonis, V. R., Gorny, M. K., Zolla-Pazner, S., Redfield, R. R., and Birx, D. L. (1994) *J. Immunol.* **153,** 449–459
45. Parren, P. W. H. I., Mondor, I., Naniche, D., Ditzel, H. J., Klasse, P. J., Burton, D. R., and Sattentau, Q. J. (1998) *J. Virol.* **72,** 3512–3519
46. Sattentau, Q., and Moore, J. P. (1995) *J. Exp. Med.* **182,** 185–196
47. Burton, D. R., Williamson, R. A., and Parren, P. W. H. I. (2000) *Virology* **270,** 1–3
48. Hart, T. K., Kirsh, R., Ellens, H., Sweet, R. W., Lambert, D. M., Petteway, S. R., Jr., Leary, J., and Bugelski, P. J. (1991) *Proc. Natl. Acad. Sci. U. S. A.* **88,** 2189–2193
49. Salzwedel, K., and Berger, E. (2000) *Proc. Natl. Acad. Sci. U. S. A.* **97,** 12794–12799
50. Burton, D. R. (1997) *Proc. Natl. Acad. Sci. U. S. A.* **94,** 10018–10023

51. Fouts, T. R., Trkola, A., Fung, M. S., and Moore, J. P. (1998) *AIDS Res. Hum. Retroviruses* **14,** 591–597
52. Nyambi, P. N., Gormy, M. K., Bastiani, L., VanderGroen, G., Williams, C., and Zolla-Pazner, S. (1998) *J. Virol.* **72,** 9384–9391
53. Stamatatos, L., Zolla-Pazner, S., Gorny, M. K., and Cheng-Mayer, C. (1997) *Virology* **229,** 360–369
54. Muster, T., Steindl, F., Purtscher, M., Trkola, A., Klima, A., Himmler, G., Rükler, F., and Katinger, H. (1993) *J. Virol.* **67,** 6642–6647
55. Moore, J. P., Cao, Y., Qing, L., Sattentau, Q. J., Pyati, J., Koduri, R., Robinson, J., Barbas, C. F., III, Burton, D. R., and Ho, D. D. (1995) *J. Virol.* **69,** 101–109
56. Sullivan, N., Sun, Y., Li, J., Hofmann, W., and Sodroski, J. (1995) *J. Virol.* **69,** 4413–4422
57. Thali, M., Furman, C., Ho, D. D., Robinson, J., Tilley, S., Pinter, A., and Sodroski, J. (1992) *J. Virol.* **66,** 5635–5641
58. Laal, S., Burda, S., Gorny, M. K., Karwowska, S., Buchbinder, A., and Zolla-Pazner, S. (1994) *J. Virol.* **68,** 4001–4008
59. McKeating, J. A., Cordell, J., Dean, C. J., and Balfe, P. (1992) *Virology* **191,** 732–742
60. Tilley, S. A., Honnen, W. J., Racho, M. E., Chou, T., and Pinter, A. (1992) *AIDS Res. Hum. Retroviruses* **8,** 461–467
61. Vijh-Warrier, S., Pinter, A., Honnen, W. J., and Tilley, S. (1996) *J. Virol.* **70,** 4466–4473
62. McKeating, J. A., McKnight, A., and Moore, J. P. (1991) *J. Virol.* **65,** 852–860
63. Staropoli, I., Chanel, C., Girard, M., and Altmeyer, R. (2000) *J. Biol. Chem.* **275,** 35137–35145
64. Yang, X., Farzan, M., Wyatt, R., and Sodroski, J. (2000) *J. Virol.* **74,** 5716–5725
65. Earl, P. L., Sugiura, W., Montefiori, D. C., Broder, C. C., Lee, S. A., Lifson, J., and Moss, B. (2001) *J. Virol.* **75,** 645–653
66. Kent, K. A., Gritz, L., Stallard, G., Cranage, M. P., Collignon, C., Thiriart, C., Corcoran, T., Silvera, P., and Stott, E. J. (1991) *AIDS* **5,** 829–836
67. Kent, K. A., Rud, E., Corcoran, T., Powell, C., Thiriart, C., Collignon, C., and Stott, E. J. (1992) *AIDS Res. Hum. Retroviruses* **8,** 1147–1151
68. Choi, W. S., Collignon, C., Thiriart, C., Burns, D. P. W., Stott, E. J., Kent, K. A., and Desrosiers, R. C. (1994) *J. Virol.* **68,** 5395–5402
69. Javaherian, K., Langlois, A. J., Montefiori, D. C., Kent, K. A., Ryan, K. A., Wymann, P. D., Stott, J., Bolognesi, D. P., Murphey-Corb, M., and Larosa, G. J. (1994) *J. Virol.* **68,** 2624–2631
70. D'Souza, M. P., Kent, K. A., Thiriart, C., Collignon, C., and Milman, G. (1993) *AIDS Res. Hum. Retroviruses* **9,** 415–422

The Stoichiometry of Trimeric SIV Glycoprotein Interaction with CD4 Differs from That of Anti-envelope Antibody Fab Fragments

Mikyung Kim, Bing Chen, Rebecca E. Hussey, Yasmin Chishti, David Montefiori, James A. Hoxie, Olwyn Byron, Gordon Campbell, Stephen C. Harrison and Ellis L. Reinherz

J. Biol. Chem. 2001, 276:42667-42676.
doi: 10.1074/jbc.M104166200 originally published online September 5, 2001
